Self-Consistent Field Theory for Melts of Low-Molecular-Weight Diblock Copolymer

ARTICLE *in* MACROMOLECULES · OCTOBER 2012

Impact Factor: 5.8 · DOI: 10.1021/ma301788q

1 AUTHOR:

Mark W Matsen
University of Waterloo
134 PUBLICATIONS **7,827** CITATIONS

Macromolecules

Article

pubs.acs.org/Macromolecules

Self-Consistent Field Theory for Melts of Low-Molecular-Weight Diblock Copolymer

M. W. Matsen*

School of Mathematical and Physical Sciences, University of Reading, Whiteknights, Reading, RG6 6AX, U.K.

ABSTRACT: This paper applies self-consistent field theory (SCFT) to discrete polymer chains consisting of a finite number of beads, N, joined together by freely jointed bonds of arbitrary potential, $b(R)$. The numerics of this SCFT can be performed efficiently using spectral or pseudospectral algorithms, permitting its application to complex morphologies. To demonstrate its effectiveness, we examine diblock copolymer melts where the polymer bonds have a fixed length, a, and the nonbonded interactions have a finite range, σ, with a strength controlled by the standard Flory–Huggins χ parameter. Although the results reduce to those of the usual SCFT for Gaussian chains in the limit of large N and small χ, there are some notable differences for short chains with strong interactions. The most significant involves the internal interfaces, which in turn affects the size of the domains. Furthermore, the finite range of the nonbonded interactions, necessary to properly treat the internal interfaces, causes a noticeable shift of the ODT toward larger χN. As χ becomes very large, particularly at small N, the finite extensibility of the freely jointed chains restricts the size of the domains, which leads to a preference for the lamellar phase.

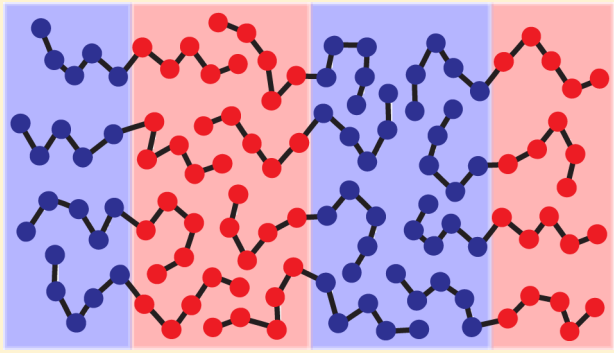

INTRODUCTION

Self-consistent field theory (SCFT)[1] has proven to be a remarkable theory for predicting the equilibrium behavior of structured polymers.[2−4] This has been well demonstrated by its success regarding diblock copolymer melts.[5] Vavasour and Whitmore[6] produced the first SCFT phase diagram, but it was limited to the classical lamellar (L), cylindrical (C) and bcc spherical (S) phases. Matsen and Schick[7] then extended it to include complex phases, predicting the gyroid (G) phase[8,9] to be more stable than the perforated-lamellar (PL) phase[10] as confirmed later by experiment.[11] In a subsequent calculation by Matsen and Bates,[12] a narrow closed-packed spherical (S_{cp}) phase was predicted along the order−disorder transition (ODT), which has since been associated with a region of densely packed spherical micelles.[13,14] Most recently, the *Fddd* (O^{70}) phase[15] was predicted by Tyler and Morse[16] and later observed in experiment.[17−19]

The standard SCFT applies mean-field theory to coarse-grained Gaussian chains, for which the statistical mechanics of a single chain in external fields is evaluated by solving a simple modified diffusion equation in three-dimensional space. This simplicity results because the polymers are treated as ideal elastic threads, where the elasticity accounts for the entropy associated with the microscopic degrees of freedom integrated out of the system by the coarse graining. However, approximating polymers by elastic threads results in a number of unphysical properties such as an unbounded end-to-end length of the molecules and a diverging entropic penalty for narrow interfaces. As such, the Gaussian chain model must be limited to situations to where the average end-to-end length of a polymer is much shorter than its contour length and where the local environment changes slowly on the monomer scale. These conditions are satisfied by polymers of high molecular weight,[20] but not necessarily by ones of low molecular weight.[21−23]

These limitations can, in principle, be overcome by applying SCFT to the worm-like chain model,[24,25] where the polymers are treated as semiflexible threads of fixed contour length. While the worm-like chain reduces to the Gaussian chain as its flexibility increases, the unphysical behavior described above is avoided so long as the rigidity of the worm-like chain remains finite. Unfortunately, the statistical mechanics of a worm-like chain in external fields involves a much more complicated diffusion equation that couples the orientation of the chain to spatial variations in the field. For simple problems where the field only varies in one direction such as the lamellar phase, the diffusion equation involves just two coordinates (one spatial and one orientational) and thus it can be readily solved.[26−28] In the general case, however, there are three spatial and two orientational coordinates, resulting in a five-dimensional diffusion equation that has so far remained numerically intractable.

Another alternative is to apply SCFT to discrete chains involving a finite number of beads joined together by freely jointed bonds. In this case, the diffusion equation is replaced by an iterative equation involving an integration over the three

Received: August 26, 2012
Revised: October 4, 2012
Published: October 11, 2012

dx.doi.org/10.1021/ma301788q | *Macromolecules* 2012, 45, 8502−8509

spatial coordinates. Although the dimensionality of the problem does not increase because the orientations of the bonds are not coupled, the triple integral is difficult to evaluate accurately in real space. Consequently, this model has so far been restricted to systems in which the fields vary in only one direction.[29,30] However, we will demonstrate that if the numerics are solved using spectral[7] or pseudospectral[31] methods, then the SCFT of freely joined chains becomes equally efficient to that of Gaussian chains. This then allows us to examine the effects of finite molecular weight on the full range of periodic morphologies exhibited by diblock copolymer melts.

THEORY

Here we formulate the freely jointed chain version of SCFT for a melt of n AB diblock copolymers, each with an A-block of N_A monomers joined to a B-block of N_B monomers giving a total polymerization of $N \equiv N_A + N_B$ and an A-monomer composition of $f = N_A/N$. We assume a uniform monomer density, ρ_0, such that the total volume of the melt is $V = nN/\rho_0$. The monomers are treated as featureless beads connected by a bonded potential, $b(R)$. The natural length of a bond, a, is given by

$$a^2 \equiv \int R^2 g(R)\, \mathrm{d}\mathbf{R} \tag{1}$$

where $g(R) \propto \exp(-b(R)/k_BT)$ is normalized so that $\int g(R)\, \mathrm{d}\mathbf{R} = 1$. Because the $N - 1$ bonds of the molecule are freely jointed, the natural end-to-end length of the entire molecule is $R_0 = a(N-1)^{1/2}$.

We specify the strength of the nonbonded interactions by the usual Flory–Huggins χ parameter, but we also include a finite range, σ, to the interactions. This is done by expressing the internal energy, U, as[5]

$$\frac{U}{nk_BT} = \frac{\chi N}{V}\int u(|\mathbf{r}-\mathbf{r}'|)\phi_A(\mathbf{r})\phi_B(\mathbf{r}')\, \mathrm{d}\mathbf{r}\, \mathrm{d}\mathbf{r}' \tag{2}$$

where $\phi_\gamma(\mathbf{r})$ is the dimensionless concentration of the γ-type monomers (γ = A or B) and $u(R)$ is selected such that $\int u(R)\, d\mathbf{R} = 1$ and

$$\sigma^2 \equiv \int R^2 u(R)\, \mathrm{d}\mathbf{R} \tag{3}$$

From the internal energy, it follows that the self-consistent conditions for the external fields acting on the A and B monomers are

$$w_A(\mathbf{r}) = \chi N \int u(R)\phi_B(\mathbf{r}-\mathbf{R})\, \mathrm{d}\mathbf{R} + \xi(\mathbf{r}) \tag{4}$$

$$w_B(\mathbf{r}) = \chi N \int u(R)\phi_A(\mathbf{r}-\mathbf{R})\, \mathrm{d}\mathbf{R} + \xi(\mathbf{r}) \tag{5}$$

respectively, where $\xi(\mathbf{r})$ is the usual pressure field that enforces incompressibility, $\phi_A(\mathbf{r}) + \phi_B(\mathbf{r}) = 1$.

The first step in SCFT involves solving the statistical mechanics of a single molecule in the external fields, $w_\gamma(\mathbf{r})$. This is done by calculating two partial partition functions, $q(\mathbf{r},i)$ and $q^\dagger(\mathbf{r},i)$ for $i = {}^1/_2, 1, {}^3/_2, ..., N + {}^1/_2$. The first one is obtained by starting from $q(\mathbf{r},1/2) = 1$ and iterating

$$q(\mathbf{r}, i) = h_\gamma(\mathbf{r})q\left(\mathbf{r}, i - \frac{1}{2}\right) \tag{6}$$

$$q\left(\mathbf{r}, i + \frac{1}{2}\right) = \int g(R)q(\mathbf{r}-\mathbf{R}, i)\, \mathrm{d}\mathbf{R} \tag{7}$$

for $i = 1, 2, ..., N$, where

$$h_\gamma(\mathbf{r}) \equiv \exp(-w_\gamma(\mathbf{r})/N) \tag{8}$$

with γ = A for $i \le N_A$ and γ = B for $i > N_A$. The complementary partition function is obtained starting from $q^\dagger(\mathbf{r},N + 1/2) = 1$ and applying the same iterations, eqs 6 and 7, but with i decreasing by a half at each step (i.e., the same equations but with $i - 1/2 \Leftrightarrow i + 1/2$). Once the partial partition functions are known, the concentration of A monomers is given by

$$\phi_A(\mathbf{r}) = \frac{V}{QN}\sum_{i=1}^{N_A} q\left(\mathbf{r}, i - \frac{1}{2}\right)q^\dagger(\mathbf{r}, i) \tag{9}$$

where the sum is over the integers $i = 1, 2, ..., N_A$ and $Q = \int q(\mathbf{r},N)\, \mathrm{d}\mathbf{r}$ is the full partition function for a single diblock copolymer in the external fields. The expression for $\phi_B(\mathbf{r})$ is the same except that the sum is over $i = N_A + 1, N_A + 2, ..., N$.

The convolutions in eqs 4, 5, and 7 would be computationally costly to perform in real space for triply periodic morphologies, but they become simple multiplications in Fourier space. Therefore, we express our periodic functions as

$$f(\mathbf{r}) = \sum_{\mathbf{k}} f(\mathbf{k})\exp(i\mathbf{k}\cdot\mathbf{r}) \tag{10}$$

where the Fourier coefficients are given by

$$f(\mathbf{k}) = \frac{1}{V}\int f(\mathbf{r})\exp(-i\mathbf{k}\cdot\mathbf{r})\, \mathrm{d}\mathbf{r} \tag{11}$$

For the nonperiodic function $g(R)$, we define the Fourier transform

$$g(k) = \int g(R)\exp(-i\mathbf{k}\cdot\mathbf{R})\, \mathrm{d}\mathbf{R} = \frac{4\pi}{k}\int_0^\infty g(R)\sin(kR)\, R\, \mathrm{d}R \tag{12}$$

where the second expression uses the fact that $g(R)$ only depends on the magnitude of $\mathbf{R}$. The Fourier transform of $u(R)$ is defined analogously. In the spectral representation, the field equations become

$$w_A(\mathbf{k}) = \chi N u(k)\phi_B(\mathbf{k}) + \xi(\mathbf{k}) \tag{13}$$

$$w_B(\mathbf{k}) = \chi N u(k)\phi_A(\mathbf{k}) + \xi(\mathbf{k}) \tag{14}$$

and $q(\mathbf{k},i)$ is obtained by iterating

$$q(\mathbf{k}, i) = \sum_{\mathbf{k}'} h_\gamma(\mathbf{k}-\mathbf{k}')q\left(\mathbf{k}', i - \frac{1}{2}\right) \tag{15}$$

$$q\left(\mathbf{k}, i + \frac{1}{2}\right) = g(k)q(\mathbf{k}, i) \tag{16}$$

from $q(\mathbf{k},1/2) = \delta_{\mathbf{k},0}$. Once this and the analogous function, $q^\dagger(\mathbf{k},i)$, have been calculated, the Fourier coefficients of the A-monomer concentration are given by

$$\phi_A(\mathbf{k}) = \frac{V}{QN}\sum_{i=1}^{N_A}\sum_{\mathbf{k}'} q\left(\mathbf{k}-\mathbf{k}', i - \frac{1}{2}\right)q^\dagger(\mathbf{k}', i) \tag{17}$$

where $Q = Vq(\mathbf{k} = 0,N)$. Again the expression for the B-monomer concentration is the same except that i is summed from $N_A + 1$ to N. The free energy is also given by a simple expression

dx.doi.org/10.1021/ma301788q | Macromolecules 2012, 45, 8502–8509

$$\frac{F}{nk_BT} = -\ln\left(\frac{Q}{V}\right) + \sum_{\mathbf{k}} [\chi N u(k)\phi_A(\mathbf{k})\phi_B(\mathbf{k}) - w_A(\mathbf{k})\phi_A(\mathbf{k}) - w_B(\mathbf{k})\phi_B(\mathbf{k})] \quad (18)$$

The last step in the SCFT calculation is to minimize the free energy with respect to the domain size, D, which is done by satisfying

$$\frac{1}{Q}\frac{\partial Q}{\partial D} - \chi N \sum_{\mathbf{k}} u'(k)\frac{\partial k}{\partial D}\phi_A(\mathbf{k})\phi_B(\mathbf{k}) = 0 \quad (19)$$

For morphologies with more than one independent length scale (e.g., PL and *Fddd*), this has to be satisfied separately for each length.

Although the use of Fourier space simplifies convolutions by transforming them into simple scalar multiplications, it actually complicates the first step of the iteration for the partial partition functions by changing it from a scalar multiplication, eq 6, to a matrix multiplication, eq 15.[32] This complication could be avoided by using a pseudospectral strategy,[31] where the first step is performed in real space with eq 6 and the second step is done in Fourier space with eq 16, using fast Fourier transforms (FFTs) to switch back and forth between the two spaces. For many problems, the pseudospectral method is faster than the full-spectral approach, but generally not when it comes to ordered periodic morphologies.[33] This is because the symmetry of a morphology is easily incorporated into the calculation greatly reducing the number of independent Fourier coefficients.[34] Therefore, we opt for the full-spectral approach using symmetrized basis functions.[12]

For weakly segregated morphologies that can be accurately represented by $\lesssim$100 basis functions, we generally use the Broyden method to solve the self-consistent field equations. If a greater number of basis functions is required, then it becomes more efficient to use the Anderson mixing method.[34] Both methods, however, have difficulty in converging to a self-consistent solution when the molecules become highly stretched, which limits the segregation to which we can solve the SCFT. Nevertheless, so long as we are able to converge on a solution, our numerical accuracy is never compromised; the inaccuracies are always smaller than the resolution of our plots.

RESULTS

This section presents the SCFT for diblock copolymers with a fixed bond length, where

$$g(R) = \frac{1}{4\pi a^2}\delta(R - a) \quad (20)$$

$$g(k) = \frac{\sin(ka)}{ka} \quad (21)$$

As such, the total contour length of each molecule is $L = a(N - 1)$, which means that a is both the statistical segment length and Kuhn length, defined by $\lim_{N\to\infty} R_0/\sqrt{N}$ and $\lim_{N\to\infty} R_0^2/\sqrt{L}$, respectively. (Note that for Gaussian chains, a is just the statistical segment length; the Kuhn length is zero because the contour length of a Gaussian chain is infinite.) For the nonbonded A/B interactions, we select the potential

$$u(R) = \frac{1}{(2\pi\sigma^2)^{3/2}}\exp\left(-\frac{R^2}{2\sigma^2}\right) \quad (22)$$

$$u(k) = \exp\left(-\frac{k^2\sigma^2}{2}\right) \quad (23)$$

In the limit $\sigma \to 0$ where the range of the interaction vanishes, $u(R)$ reduces to a Dirac delta function resulting in the usual contact force normally used in SCFT.

To begin, we first illustrate the importance of having a finite range for the A/B interactions. This is done in Figure 1, where

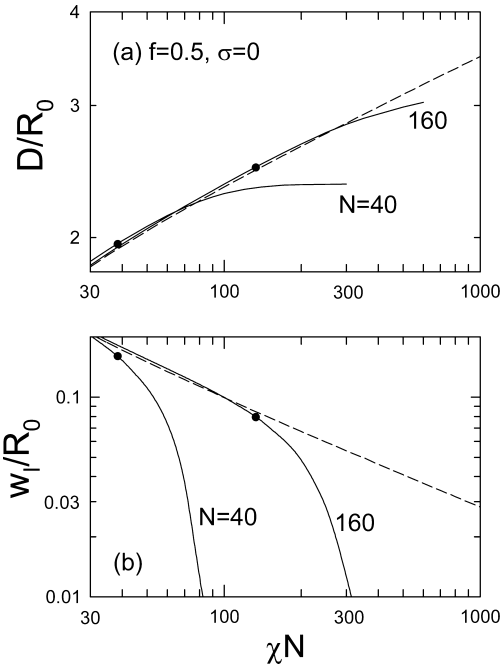

Figure 1. (a) Period and (b) interfacial width of the lamellar (L) phase for symmetric diblock copolymers with simple contact forces between the A and B monomers. The dots denote the points where $w_I = a$. The dashed curves are calculated with the Gaussian chain model, which corresponds to the $N \to \infty$ limit.

we compare predictions for the period, D, and interfacial width, w_I, of the lamellar (L) phase calculated for Gauusian chains and freely jointed chains with the interaction range set to $\sigma = 0$. (The width of the interface is defined by $w_I = |\phi_A'(z_I)|^{-1}$ where its location, z_I, is specified by $\phi_A(z_I) = 1/2$.) The results for the freely jointed chains (solid curves) closely follow those for Gaussian chains (dashed curves),[35] but only while the interfacial width remains $w_I \gtrsim a$. Beyond these points, denoted by solid dots, the interfacial width for the freely jointed chains rapidly narrows and the period plateaus. This is because there is no entropic penalty for further narrowing of the interface once the two unlike monomers at the diblock junction (i.e., $i = N_A$ and $i = N_A + 1$) are able to simultaneously reside in the relatively pure regions of their respective domains. Likewise, there is no further advantage for reducing the interfacial area per molecule, and thus the domain size ceases to increase.

The root of the problem that leads to the unphysical behavior in Figure 1 is that the unlike monomers, even those at the diblock junctions, are able to avoid unfavorable contact once $w_I \lesssim a$. Of course, this should not happen since real nonbonded interactions have a finite range, σ, similar to the bond length, a, and thus the unfavorable interactions should extend across the narrow interfaces. In Figure 2, we repeat the calculation again, but with the interaction range set to $\sigma = a$. Now that the unlike monomers are unable to avoid unfavorable

dx.doi.org/10.1021/ma301788q | Macromolecules 2012, 45, 8502−8509

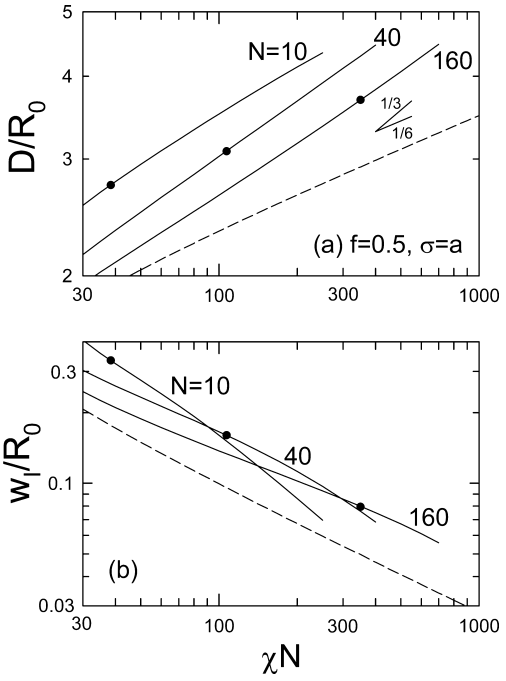

Figure 2. Analogous plots to those of Figure 1, but with finite-range, $\sigma = a$, interactions between the A and B monomers. The straight-line segments in part a show the slopes corresponding to $D \propto \chi^{1/3}$ and $D \propto \chi^{1/6}$ scaling.

interactions across the interface, the interfacial width decreases gradually and the period continues to increase with χ. In fact, the rate of increase becomes substantially faster than that of Gaussian chains for which $D \sim \chi^{1/6}$. The exponent for the freely jointed chains seems to approach 1/3 beyond the points where the interface is narrower than the bond length (denote by solid dots). The short $N = 10$ diblocks are an exception, but this is because they are becoming fully stretched.

Unlike for Gaussian chains, the lamellar phase for freely jointed chains has a maximum period of $D_{max} = 2L$ due to the finite length, L, of the molecules. To gauge the degree of chain stretching in Figure 2, we evaluate $D_{max}/R_0 = 2(N-1)^{1/2}$ to be 6.0, 12.49, and 25.22 for $N = 10$, 40 and 160, respectively. Hence, the short $N = 10$ diblocks in Figure 2 are indeed approaching their full extension, whereas the two longer molecules are not. The extension of the $N = 10$ diblocks is further illustrated in Figure 3, where we plot the concentration profiles of the individual A monomers for three consecutive values of χ. By $\chi = 20$, the separation between the adjacent peaks is nearly a implying that the bonds are perpendicular to the lamellae.

Although the details of the model modify the scaling of D with respect to χ, this does not alter the scaling with respect to N. The discreteness of the freely jointed chains affects the interface and its tension, but nevertheless the properties of the interface should become independent of N in the high-molecular-weight limit. Thus, the usual $D \sim N^{2/3}$ scaling predicted by strong-stretching theory (SST)[36] must continue to hold at large N, since all it assumes is a fixed interfacial tension. Figure 4 confirms that D does indeed increase as $N^{2/3}$, and that the width (and presumably all other features) of the interface become independent of N.

The advantage of the freely jointed chain model, as compared to for example the worm-like chain model, is that

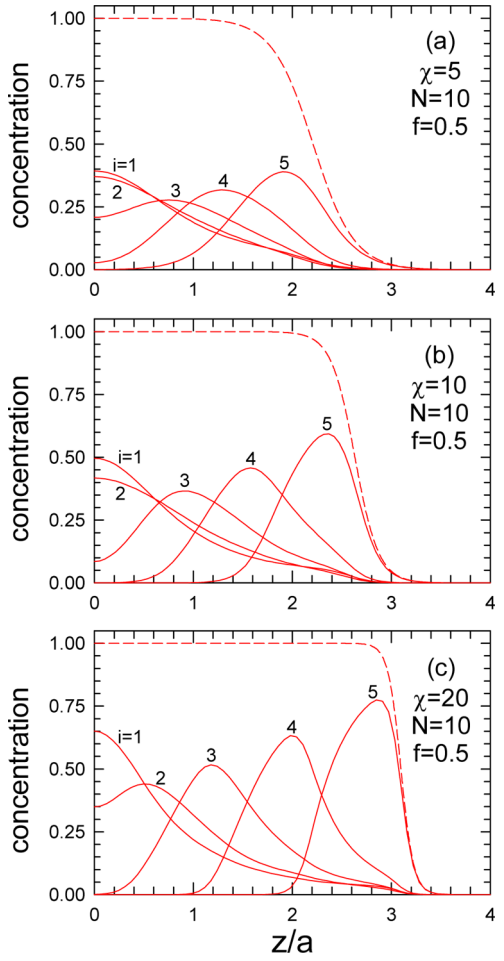

Figure 3. Concentration profiles of the individual A-type monomers in the lamellar (L) phase of a symmetric $N = 10$ diblock copolymer melt, plotted at several values of χ. The dashed curves show the combined concentrations, ϕ_A.

the SCFT can be readily solved for complex morphologies. We illustrate this fact by calculating the full phase diagrams for $N = 40$ and 80 in Figure 5. Although the discreteness of the freely jointed chain model has a considerable impact on the internal interfaces causing a substantial rise in interfacial tension and thus larger domains, all the ordered phases are affected to a similar extent. Consequently, the topology of the phase diagram is unaffected. In particular, the gyroid (G) phase remains the most stable of the complex phases, apart from the *Fddd* (O^{70}) phase at weak segregations.

The main effect of finite N is to produce an upward shift in the phase boundaries, as demonstrated in Figure 6a where we plot the position of the phase boundaries at $f = 0.4$ as a function of N. In order to ascertain the source of this shift, we repeat the calculation in Figure 6b but this time with only contact forces (i.e., $\sigma = 0$). Evidently the shift is due to the finite range of the nonbonded interactions, given that it vanishes as $\sigma \to 0$. In fact, without the finite range, there is a slight downward shift, but this only becomes noticeable for $N \lesssim 30$.

At the weak to intermediate levels of segregation in Figures 5 and 6, the diblock copolymers are not stretched enough for the differences between freely jointed and Gaussian chains to become appreciable. However, considerable differences are certain to emerge in the strong-segregation regime as the freely jointed chains start to become fully stretched. To illustrate this,

dx.doi.org/10.1021/ma301788q | *Macromolecules* 2012, 45, 8502−8509

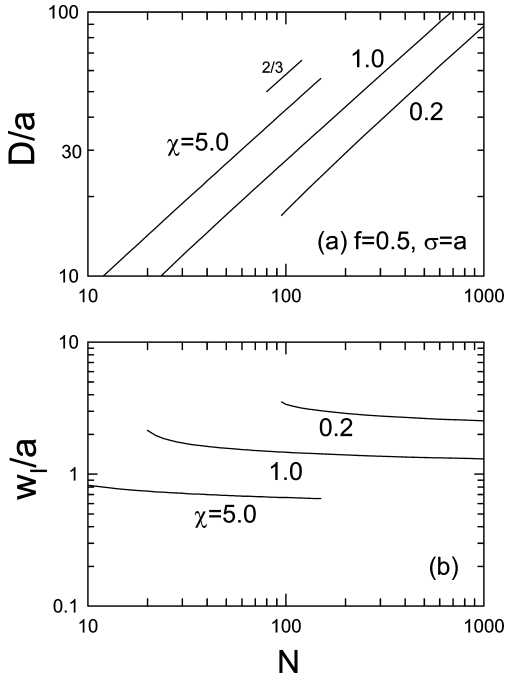

Figure 4. (a) Period and (b) interfacial width of the lamellar (L) phase for symmetric diblock copolymers. The short line segment in part a denotes the slope corresponding to $D \sim N^{2/3}$ scaling.

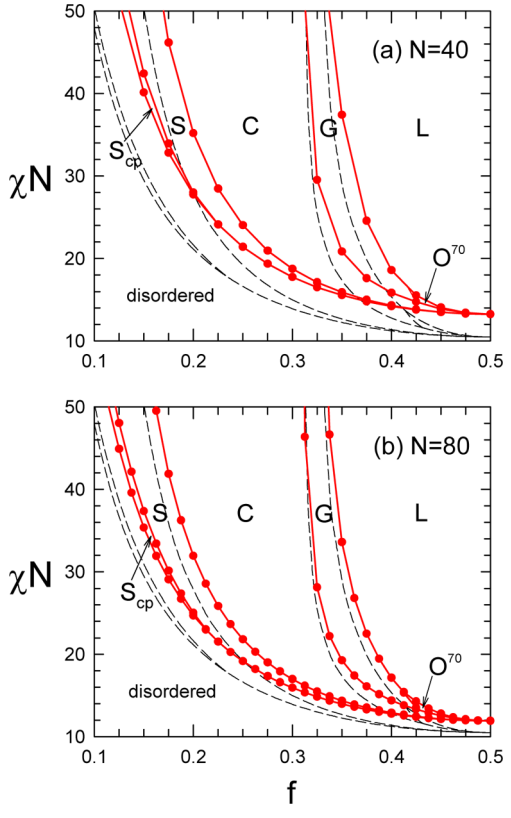

Figure 5. Phase diagrams for freely jointed diblock copolymers of (a) $N = 40$ and (b) $N = 80$ monomers, showing the stability regions of the ordered lamellar (L), cylindrical (C), bcc spherical (S), hcp spherical (S_{cp}), gyroid (G) and *Fddd* (O^{70}) morphologies. The dashed curves, obtained using the Gaussian chain model, correspond to the $N \rightarrow \infty$ limit.

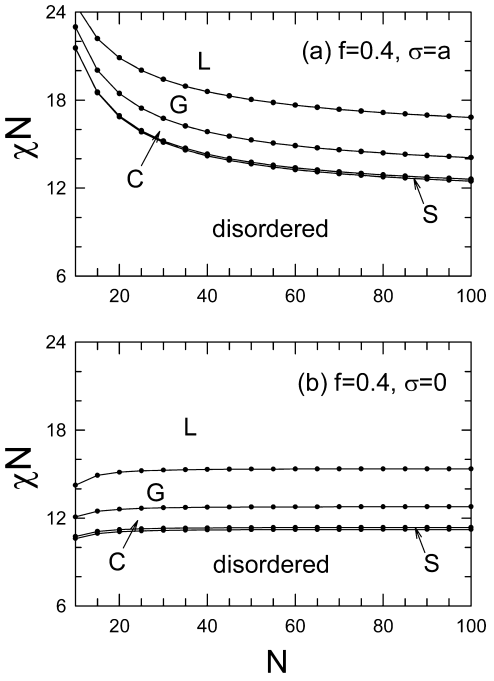

Figure 6. Phase boundaries for asymmetric $f = 0.4$ diblock copolymers with (a) finite-range interactions, σ = a, and (b) simple contact forces, $\sigma = 0$. Note that the bcc spherical (S) regions are difficult to resolve on this scale.

Figure 7 compares the free energies of the lamellar (L) and cylindrical (C) phases up to large χN for asymmetric $f = 0.3$

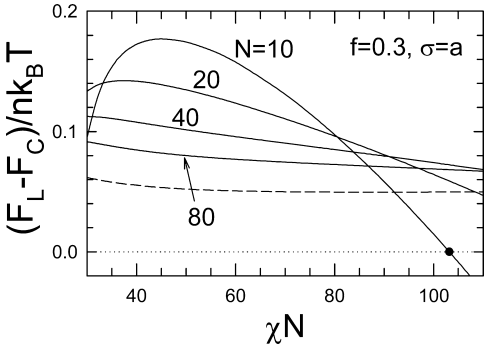

Figure 7. Free energy difference between the lamellar (L) and cylinder (C) phases of asymmetric $f = 0.3$ diblock copolymers of various polymerizations. The dashed curve, obtained using the Gaussian chain model, corresponds to the $N \rightarrow \infty$ limit.

diblock copolymers of various polymerizations, N. (The gyroid (G) phase is omitted from this calculation because of its high computational cost at these levels of segregation.) For Gaussian chains (dashed curve), the C phase remains stable up to $\chi N \rightarrow \infty$.[36,37] For the freely jointed chains (solid curves), however, the C phase becomes less stable as the segregation increases, particularly as N becomes small. In the case of $N = 10$, the stability of L overtakes that of C at $\chi N = 103.19$, and presumably the same happens for the larger values of N at higher values of χN.

In order to explain the transition from C to L, Figure 8 plots the monomer distributions in the C and L phases for the $N = 10$ diblock copolymers at the point where their free energies are equal. In the C phase, the minority A blocks (red curves) are

dx.doi.org/10.1021/ma301788q | *Macromolecules* 2012, 45, 8502–8509

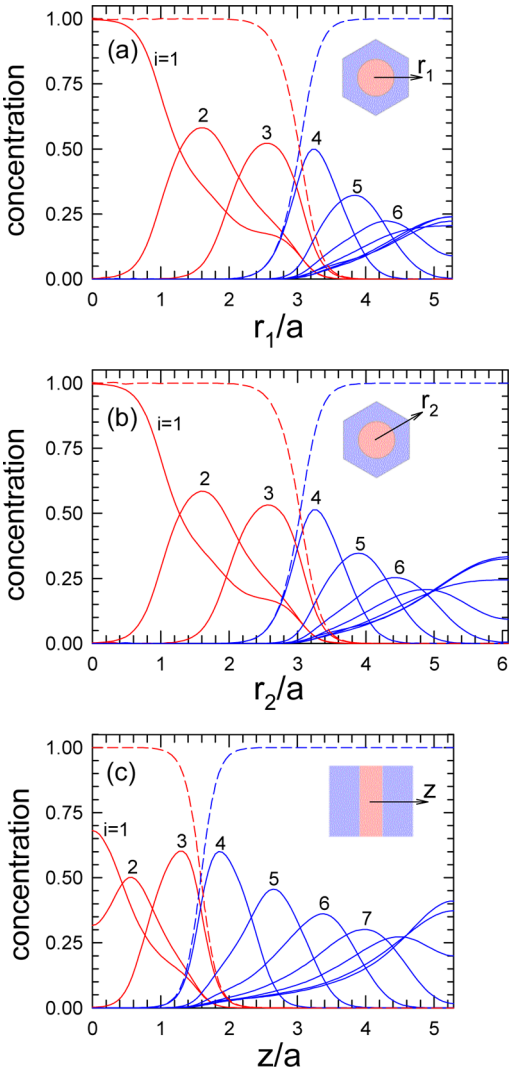

Figure 8. Concentration profiles for the 3 A-type (red) and 7 B-type (blue) monomers of an asymmetric $N = 10$ diblock copolymer in the coexisting lamellar (L) and cylinder (C) phases at $\chi N = 103.19$. The dashed curves show the combined concentrations, ϕ_A and ϕ_B. The top plots are for two different paths through the C phase, and the bottom plot is for the L phase.

highly stretched, almost to their fully extended length. This limits the radius of the cylinders to approximately $3a$, which in turn restricts the size of the whole unit cell through the incompressibility constraint. Indeed the ratio of the nearest-neighbor distances between cylinders and lamellae is 0.997 for the $N = 10$ freely joint chains, whereas the ratio is 1.049 for Gaussian chains at the same value of χN. The only way that the system can continue to increase the domain size so as to reduce interface area is to switch to the L phase.

DISCUSSION

We have shown that SCFT can be applied to freely jointed chains as easily as it can to the usual Gaussian chains. Although we have referred to the beads of the freely jointed chain as individual chemical monomers albeit without any atomic detail, it is more accurate to regard them as Kuhn segments. Each Kuhn segment will generally contain a few chemical units (the actual number depends on the chain flexibility) and thus a freely jointed chain is still a coarse-grained model, just not to the same extent as a Gaussian chain. A Gaussian segment needs to have about 10 Kuhn segments in order to acquire its elastic behavior.[3] Because the level of coarse graining is less, the freely jointed chain model has a greater range of applicability. As always though, there is a price to pay for this, which is the increased number of parameters. For instance, the behavior of the freely jointed chains depends on the individual values of χ and N, rather than just their product.

The most stringent restriction on the validity of the Gaussian chain model is that the interfacial width should remain large relative to the segment size. As we have seen, inaccuracies in the treatment of the interfacial region indirectly impact the domain size. This follows from the strong-segregation theory (SST),[36] which predicts the period of the lamellar phase to be

$$D = 2a\left(\frac{4N^2\Gamma_I}{\pi^2}\right)^{1/3} \tag{24}$$

in the $N \to \infty$ limit, where $\Gamma_I \equiv \gamma_I/k_BTa\rho_0$ is a dimensionless measure of the interfacial tension, γ_I. For Gaussian chains, the dimensionless tension is approximately

$$\Gamma_I = \frac{\chi w_I}{4a} + \frac{a}{6w_I} = \sqrt{\frac{\chi}{6}} \tag{25}$$

where the first term is the enthalphic penalty of mixing unlike segments and the second term is the entropic penalty of stretching chains across the interface. Their combination is minimized by an interfacial width of $w_I = 2a/(6\chi)^{1/2}$ resulting in $\Gamma_I \sim \chi^{1/2}$, which in turn leads to the usual $D \sim a\chi^{1/6}N^{2/3}$ scaling for the domain size. Fitting the curves in Figure 4a to eq 24 gives $\Gamma_I = 0.21$, 0.66, and 2.41, while eq 25 predicts $\Gamma_I = 0.18$, 0.41, and 0.91 for $\chi = 0.2$, 1.0, and 5.0, respectively. Although there is reasonable agreement at small χ, eq 25 gradually becomes invalid as the interface narrows. This is because the entropic penalty no longer increases once the interface is narrower than the Kuhn length.

The freely jointed chain model does continue to treat the interface properly for $w_I < a$, but only if the nonbonded interactions have a finite range. Once the entropic penalty in eq 25 ceases too increase, it becomes necessary to account for the fact that the unlike monomers cannot avoid interacting by simply letting $w_I \to 0$. With our current choice of $u(R)$, the enthalpic penalty of an infinitely sharp interface becomes

$$\frac{U}{nk_BT} = \frac{2\chi N}{D}\int_{z'=-\infty}^{0}\int_{z=0}^{\infty}\frac{\exp((z-z')^2/2\sigma^2)}{\sqrt{2\pi\sigma^2}}\,dz\,dz' = \frac{\sigma\chi N}{D}\sqrt{\frac{2}{\pi}} \tag{26}$$

which remains positive so long as $\sigma > 0$. If we use this to approximate the enthalpic penalty and assume that the entropic penalty is relatively insignificant, then we get an interfacial tension of

$$\Gamma_I = \frac{\sigma\chi}{a\sqrt{2\pi}} \tag{27}$$

This implies that the domain size should scale as $D \sim a\chi^{1/3}N^{2/3}$ once $w_I \ll a$, so long as the chains are not too extended so as to invalidate eq 24. Indeed, the results in Figure 2a show that the exponent of χ increases from 1/6 toward 1/3 as the interface narrows, apart from the one example for $N = 10$ where the diblocks are highly extended. Returning to the case of $\chi = 5.0$

dx.doi.org/10.1021/ma301788q | Macromolecules 2012, 45, 8502−8509

with $\sigma = a$, eq 27 now predicts $\Gamma_I = 1.99$, which is much closer to the value of $\Gamma_I = 2.41$ extracted from Figure 4a. The prediction is still a bit too small, partly because eq 26 underestimates the enthalpy and partly because we ignored the entropic penalty.[38]

According to SST,[36] the free energy of a strongly segregated morphology scales as $F \sim \Gamma_I^{2/3}$ regardless of its geometry, and thus the relative stability of the ordered phases should not be significantly affected by changes in Γ_I. Indeed, the position of the complex phase region in Figure 5 is reasonably insensitive to N in the intermediate-segregation regime, but there is a sizable shift of the ODT at weak segregations. As we have already seen in Figure 6, the upward shift in the ODT results from the finite range, σ, of the nonbonded interactions. In the weak-segregation regime, concentration profiles are well approximated by the first harmonics of the principle wave-vector, k^*. Consequently, the finite range simply reduces the fields, eqs 13 and 14, by a factor of $u(k^*)$, which must then be compensated for by an increase in χN in order to induce the ODT. At $f = 0.5$, this implies

$$(\chi N)_{\mathrm{ODT}} \approx 10.495 \exp((k^*\sigma)^2/2) = 10.495 \exp(11.35/N) \tag{28}$$

where we have used the RPA predictions, $(\chi N)_{\mathrm{ODT}} = 10.495$ and $k^* a N^{1/2} = 4.765$, for Gaussian chains.[39] Eq 28 predicts $(\chi N)_{\mathrm{ODT}} = 12.09$ for freely jointed chains of $N = 80$, which agrees well with the actual value 11.92 from Figure 5b. For the shorter $N = 40$ chains, the prediction $(\chi N)_{\mathrm{ODT}} = 13.94$ is naturally less accurate, but it is still close to the value 13.25 obtained from Figure 5a.

Although the behavior of the freely jointed chains has remained surprisingly similar to that of Gaussian chains in the weak to intermediate segregation regimes, things will certainly become very different as $\chi \to \infty$. This is because the fixed contour length of the freely jointed chains limits their extension and thus restricts the domain size, whereas Gaussian chains can be extended indefinitely allowing the domain size to diverge. Admittedly it takes an exceptionally large χ for the freely jointed chains to approach their full extension, even when N is as small as 10. Nevertheless, as this happens, they will begin to behave as rods (i.e., liquid-crystalline molecules), and therefore they will at some point self-assemble into the lamellar (i.e., smectic-C) phase regardless of their composition, f.

We can now estimate the conditions under which our freely jointed chain model reduces to the Gaussian chain model. Polymeric behavior presumably requires the diblock copolymers to have 10−20 coarse-grained segments, which must each contain at least 10 beads as explained above. This turns out to be about the same number of beads necessary for us to ignore the finite range of the nonbonded interactions. Assuming $\sigma \approx a$, eq 28 requires $N \gtrsim 200$ for the shift in the ODT of symmetric diblocks to be $\lesssim$5%. Lastly, we must ensure that the Gaussian estimate of the interfacial width, $w_I = 2a/(6\chi)^{1/2}$, is at least a couple Kuhn lengths, which requires $\chi \lesssim 0.2$. Significant deviations from the Gaussian chain model should only occur when one or both of these conditions are violated.

The SCFT for freely jointed chains is exceptionally versatile. Not only can the calculation be performed for arbitrary potentials, $b(R)$ and $u(R)$, between bonded and nonbonded monomers, respectively, one could also allow for different potentials between the different monomer types. For instance, the A−A and B−B bonds could be assigned different lengths, which would result in conformational asymmetry.[40] The strict incompressibility condition, $\phi_A(\mathbf{r}) + \phi_B(\mathbf{r}) = 1$, may not be particularly appropriate at the monomer length scale, but there is no problem to relax this constraint. One can easily introduce a finite compressibility,[5] although it adds another parameter to the model.

We should point out that the R dependence in the potentials, $b(R)$ and $u(R)$, refers to the center-to-center distance between monomers. Furthermore, $\phi_\gamma(\mathbf{r})$ is the distribution of the monomer centers as opposed to the actual concentration of material. The concentration of material, assuming spherical monomers, is given by the convolution[30]

$$\bar{\phi}_\gamma(\mathbf{r}) = \int \rho(R)\phi_\gamma(\mathbf{r} - \mathbf{R})\, \mathrm{d}\mathbf{R} \tag{29}$$

where $\rho(R)$ is the individual monomer profile normalized such that $\int \rho(R)\, \mathrm{d}\mathbf{R} = 1$. Rather than including a finite-range interaction, $u(R)$, between nonbonded monomers, we could have instead replaced $\phi_\gamma(\mathbf{r})$ by $\bar{\phi}_\gamma(\mathbf{r})$ in the usual SCFT expressions[2] for the internal energy, U, and the self-consistent fields, $w_\gamma(\mathbf{r})$. However, this ends up being exactly equivalent to what we have done. In Fourier space, $\bar{\phi}_\gamma(\mathbf{k}) = \rho(k)\phi_\gamma(\mathbf{k})$, and so it follows that this modification simply corresponds to the substitution $u(k) \Rightarrow \rho^2(k)$. Even switching the incompressibility condition to $\bar{\phi}_A(\mathbf{r}) + \bar{\phi}_A(\mathbf{r}) = 1$ changes nothing, provided that both monomer types have the same profile, $\rho(R)$. This is because, in Fourier space, the alternative incompressibility condition becomes $\rho(k)[\phi_A(\mathbf{k}) + \phi_B(\mathbf{k})] = 0$ for $\mathbf{k} \neq 0$, which equates to our present condition given that $\rho(k) \neq 0$.

Because of its computational tractability, the standard SCFT is often used to model systems of surfactant or lipid molecules,[41−44] even though these small molecules are clearly not large enough to justify the coarse-grained Gaussian chain model. It is far more sensible, for example, to model a phospholipid of a biological membrane as two short freely jointed chains, representing the hydrocarbon tails, connected to a large sphere, representing the polar headgroup. Although the hydrocarbon tails could be treated even more realistically by assigning a bending energy to the bonds, the iterative equations for the partial partition functions would then involve integrations over the bond orientations.[45] Provided one sticks with freely jointed bonds, the calculation would remain as simple as that of the standard SCFT. In fact, if the calculation was being done pseudospectrally, then it would just be a trivial modification to switch from Gaussian chains to freely jointed chains. Furthermore, the computational cost would be greatly reduced, because the modified diffusion equation for Gaussian chains can require hundreds of FFTs for an accurate solution[33] whereas the iterative equations for freely jointed chains, eqs 6 and 16, only require two FFTs per bead. Given the huge numerical advantage, researchers might also consider using short freely jointed chains for computationally challenging polymeric problems, especially since their behavior is much the same as that of Gaussian chains.

SUMMARY

We have performed self-consistent field theory (SCFT) for melts of AB diblock copolymer, where the molecules are modeled as freely jointed chains with a finite number of beads, N, joined together by bonds of fixed length, a, and where the nonbonded interactions between A and B beads have a finite range, σ. The freely jointed chains are more appropriate for low-molecular-weight polymers than the usual Gaussian chains,

and they may even provide a reasonable model for surfactant or lipid molecules. Although the SCFT for freely jointed chains involves a number of convolutions, which are computational costly to evaluate in real space for multidimensional morphologies, they become simple multiplications in Fourier space. Consequently, the SCFT can be applied to freely jointed chains as readily as it can to Gaussian chains, and in fact the use of freely jointed chains can greatly reduce the numerical cost of SCFT calculations, which would be particularly useful for computational challenging problems.

The most significant consequence of using freely jointed chains instead of Gaussian chains is the χ-dependence of the interfacial tension and its effect on domain size, D. With freely jointed chains and finite-range interactions, the usual $D \sim \chi^{1/6}$ scaling gradually switches to $D \sim \chi^{1/3}$ as the interfaces become narrow relative to the Kuhn length. Nevertheless, the standard $D \sim N^{2/3}$ scaling still holds in the limit of large N regardless of how narrow the interfaces are. Since changes in interfacial tension affect all well-ordered morphologies similarly, the phase diagram is relatively unaffected by the discreteness of the freely jointed chain in the intermediate-segregation regime. The finite range of the nonbonded interactions does, however, affect the weakly segregated phases, shifting the phase boundaries toward higher χN. In the strong-segregation limit, the finite extensibility of the freely jointed chains eventually limits the size of the minority domains, forcing diblock copolymers to adopt the lamellar morphology regardless of their asymmetry. On the basis of our calculations, these finite molecular-weight effects will remain quantitatively significant for copolymers with $N \lesssim 200$ Kuhn segments or with strong interactions of $\chi \gtrsim 0.2$.

AUTHOR INFORMATION

Corresponding Author

*E-mail: m.w.matsen@reading.ac.uk.

Notes

The authors declare no competing financial interest.

ACKNOWLEDGMENTS

This work was funded by the EPSRC (Grant No. EP/G026203/1).

REFERENCES

(1) Edwards, S. A. *Proc. Phys. Soc. London* **1965**, *85*, 613−624.
(2) Matsen, M. W. *J. Phys.: Condens. Matter* **2002**, *14*, R21−R47.
(3) Matsen, M. W. In *Soft Matter: Polymer Melts and Mitures*; Gompper, G., Schick, M., Eds.; Wiley-VCH: Weinheim, Germany, 2006; Vol. *1*, Chapter 2.
(4) Fredrickson, G. H. *The Equilibrium Theory of Inhomogeneous Polymers*; Oxford University Press: New York, 2006.
(5) Helfand, E. *J. Chem. Phys.* **1975**, *62*, 999−1005.
(6) Vavasour, J. D.; Whitmore, M. D. *Macromolecules* **1992**, *25*, 5477−5486.
(7) Matsen, M. W.; Schick, M. *Phys. Rev. Lett.* **1994**, *72*, 2660−2663.
(8) Schulz, M. F.; Bates, F. S.; Almdal, K.; Mortensen, K. *Phys. Rev. Lett.* **1994**, *73*, 86−89.
(9) Hajduk, D. A.; Harper, P. E.; Gruner, S. M.; Honeker, C. C.; Kim, G.; Thomas, E. L. *Macromolecules* **1994**, *27*, 4063−4075.
(10) Hamley, I. W.; Koppi, K. A.; Rosedale, J. H.; Bates, F. S.; Almdal, K.; Mortensen, K. *Macromolecules* **1993**, *26*, 5959−5970.
(11) Hajduk, D. A.; Takenouchi, H.; Hillmyer, M. A.; Bates, F. S.; Vigild, M. E.; Almdal, K. *Macromolecules* **1997**, *30*, 3788−3795.
(12) Matsen, M. W.; Bates, F. S. *Macromolecules* **1996**, *29*, 1091−1098.
(13) Schwab, M.; Stühn, B. *Colloid Polym. Sci.* **1997**, *275*, 341−351.
(14) Han, C. D.; Vaidya, N. Y.; Kim, D.; Shin, G.; Yamaguchi, D.; Hashimoto, T. *Macromolecules* **1998**, *33*, 3767−3780.
(15) Bailey, T. S.; Hardy, C. M.; Epps, T. H.; Bates, F. S. *Macromolecules* **2002**, *35*, 7007−7017.
(16) Tyler, C. A.; Morse, D. C. *Phys. Rev. Lett.* **2005**, *94*, 208302.
(17) Takenaka, M.; Wakada, T.; Akasaka, S.; Nishitsuji, S.; Saijo, K.; Shimizu, H.; Kim, M. I.; Hasegawa, H. *Macromolecules* **2007**, *40*, 4399−4402.
(18) Kim, M. I.; Wakada, T.; Akasaka, S.; Nishitsuji, S.; Saijo, K.; Hasegawa, H.; Ito, K.; Takenaka, M. *Macromolecules* **2008**, *41*, 7667−7670.
(19) Kim, M. I.; Wakada, T.; Akasaka, S.; Nishitsuji, S.; Saijo, K.; Hasegawa, H.; Ito, K.; Takenaka, M. *Macromolecules* **2009**, *42*, 5266−5271.
(20) Bates, F. S.; Schulz, M. F.; Khandpur, A. K.; Förster, S.; Rosedal, J. H.; Almdal, K.; Mortensen, K. *Faraday Discuss.* **1994**, *98*, 7−18.
(21) Hillmyer, M. A.; Bates, F. S. *Macromolecules* **1996**, *29*, 6994−7002.
(22) Schmidt, S. C.; Hillmyer, M. A. *J. Polym. Sci., Part B* **2002**, *40*, 2364−2376.
(23) Wolf, J. H.; Hillmyer, M. A. *Langmuir* **2003**, *19*, 6553−6560.
(24) Kratky, O.; Porod, G. *Rec. Trav. Chim.* **1949**, *68*, 1106−1123.
(25) Saito, N.; Takahashi, K.; Yunoki, Y. *J. Phys. Soc. Jpn.* **1967**, *22*, 219−226.
(26) Morse, D. C.; Fredrickson, G. H. *Phys. Rev. Lett.* **1994**, *73*, 3235−3238.
(27) Matsen, M. W. *J. Chem. Phys.* **1996**, *104*, 7758−7764.
(28) Deng, M.; Jiang, Y.; Liang, H. J.; Chen, J. Z. Y. *Macromolecules* **2010**, *43*, 3455−3464.
(29) Matsen, M. W.; Kim, J. U.; Likhtman, A. E. *Eur. Phys. J. E* **2009**, *29*, 107−115.
(30) Romeis, D.; Merlitz, H.; Sommer, J.-U. *J. Chem. Phys.* **2012**, *236*, 044903.
(31) Rasmussun, K., Ø.; Kalosakas, G. *J. Polym. Sci., Part B* **2002**, *40*, 1777−1783.
(32) We obtain the two transfer matrices, $h_\gamma(\mathbf{k}-\mathbf{k}')$ for γ = A and B, by solving the diffusion equation that usually occurs in SCFT but with the Laplacian term removed.
(33) Stasiak, P.; Matsen, M. W. *Eur. Phys. J. E* **2011**, *34*, 110.
(34) Matsen, M. W. *Eur. Phys. J. E* **2009**, *30*, 361−369.
(35) Matsen, M. W.; Bates, F. S. *Macromolecules* **1996**, *29*, 7641−7644.
(36) Semenov, A. E. *Sov. Phys. JETP* **1985**, *85*, 733−742.
(37) Matsen, M. W. *Eur. Phys. J. E* **2010**, *33*, 297−306.
(38) The entropic contribution missing from eq 27 should be approximately 1/6, assuming that it ceases to increase from the expression in eq 25 once $w_I < a$.
(39) Leibler, L. *Macromolecules* **1980**, *13*, 1602−1617.
(40) Matsen, M. W.; Bates, F. S. *J. Polym. Sci., Part B* **1997**, *35*, 945−952.
(41) Katsov, K.; Müller, M.; Schick, M. *Biophys. J.* **2004**, *87*, 3277−3290.
(42) Lauw, Y.; Kovalenko, A.; Stepanova, M. *J. Phys. Chem. B* **2008**, *112*, 2119−2127.
(43) Santo, K. P.; Kovalenko, A.; Stepanova, M. *Macromol. Theor. Simul.* **2010**, *19*, 228−239.
(44) Greenall, M.J .; Gompper, G. *Macromolecules* **2012**, *45*, 525−535.
(45) Schmid, F.; Schick, M. *J. Chem. Phys.* **1995**, *102*, 2080−2091.